Acta Oceanol. Sin., 2019, Vol. 38, No. 7, P. 74–83
https://doi.org/10.1007/s13131-019-1459-z
http://www.hyxb.org.cn
E-mail: hyxbe@263.net

Sensitivity of WRF simulated typhoon track and intensity over the South China Sea to horizontal and vertical resolutions

Zhiyuan Wu[1, 2, 3, 4], Changbo Jiang[1, 2*], Bin Deng[1, 2], Jie Chen[1, 2], Xiaojian Liu[4]

[1] School of Hydraulic Engineering, Changsha University of Science & Technology, Changsha 410114, China

[2] Key Laboratory of Water-Sediment Sciences and Water Disaster Prevention of Hunan Province, Changsha 410114, China

[3] School for Marine Science and Technology, University of Massachusetts Dartmouth, New Bedford, MA 02744, USA

[4] Key Laboratory of the Pearl River Estuarine Dynamics and Associated Process Regulation, Ministry of Water Resources, Guangzhou 510611, China

Received 26 January 2019; accepted 22 February 2019

Abstract

To determine the grid resolutions of the WRF model in the typhoon simulation, some sensitivity analysis of horizontal and vertical resolutions in different conditions has been carried out. Different horizontal resolutions (5, 10, 20, 30 km), nesting grids (15 and 5 km), different vertical resolutions (35-layers, 28-layers, 20-layers) and different top maximum pressures (1 000, 2 000, 3 500, 5 000 Pa) had been used in the mesoscale numerical model WRF to simulate the Typhoon Kai-tak. The simulation results of typhoon track, wind speed and sea level pressure at different horizontal and vertical resolutions have been compared and analyzed. The horizontal and vertical resolutions of the model have limited effect on the simulation effect of the typhoon track. Different horizontal and vertical resolutions have obvious effects on typhoon strength (defined by wind speed) and intensity (defined by sea level pressure, SLP), especially for sea level pressure. The typhoon intensity simulated by the high-resolution model is closer to the real situation and the nesting grids can improve computational accuracy and efficiency. The simulation results affected by vertical resolution using 35-layers is better than the simulation results using 20-layers and 28-layers simulations. Through comparison and analysis, the horizontal and vertical resolutions of WRF model are finally determined as follows: the two-way nesting grid of 15 and 5 km is comprehensively determined, and the vertical layers is 35-layers, the top maximum pressure is 2 000 Pa.

Key words: sensitivity analysis, typhoon track and intensity, horizontal and vertical resolutions, Typhoon Kai-tak, WRF

Citation: Wu Zhiyuan, Jiang Changbo, Deng Bin, Chen Jie, Liu Xiaojian. 2019. Sensitivity of WRF simulated typhoon track and intensity over the South China Sea to horizontal and vertical resolutions. Acta Oceanologica Sinica, 38(7): 74–83, doi: 10.1007/s13131-019-1459-z

1 Introduction

Typhoon is a devastating natural disaster that has long been a focus of attention in the field of atmospheric and oceanic research (Sun et al., 2017; Weng and Hsu, 2017; Wu et al., 2018, 2019a, b, c). With the rapid development of computers, typhoon numerical simulation is increasingly developed (Wang and Wang, 2014), and the model resolution is getting higher and higher (Hendricks et al., 2016; Jun et al., 2017). However, the integral calculation of the numerical model often cannot accurately describe the atmospheric motion close to the grid or the sub-grid scales. Usually, the various physical processes of these sub-grid scales (such as radiation, cumulus convection, boundary layer, etc.) need a parameterization scheme to describe (Hendricks et al., 2016; Weng and Hsu, 2017; Li et al., 2018). At the same time, the track and intensity changes of the typhoon are the results of the interaction of multi-scale meteorological systems, such as the interaction between the occurrence and development of the sub-grid process and the large-scale background environment (Hendricks et al., 2016; Jun et al., 2017; Guo and Zhong, 2017). Therefore, using different grid resolutions in typhoon numerical simulations may produce different simulation results.

In the past three decades, scholars have done a lot of research on the effects of different horizontal resolutions on the simulation effects of meteorological systems. The squall line simulation at different horizontal resolutions (1 km to 12 km) was carried out by Weisman (Weisman et al., 1997). The simulation results show that there are significant differences in the mesoscale circulation and convective structure of the squall line at different horizontal resolutions, and it is pointed out that because the coarse grid cannot describe the non-hydrostatic process.

Different horizontal resolutions were performed to analyze the simulation effects of the storm process occurring in the basin (Knutson et al., 2010; Bacmeister et al., 2018; Gettelman et al., 2018). The results show that different horizontal resolutions have a great influence on the simulation effect of precipitation. Increasing the horizontal resolution of the model can improve the forecasting results. However, the higher resolution model simu-

Foundation item: The National Natural Science Foundation of China under contract Nos 51809023, 51839002 and 51879015; the Open Research Foundation of the Key Laboratory of the Pearl River Estuarine Dynamics and Associated Process Regulation, the Ministry of Water Resources under contract No. 2018KJ03.

*Corresponding author, E-mail: jiangchb@csust.edu.cn

lates a stronger precipitation intensity, and different resolutions have little effect on the simulation effect of the circulation situation.

Davis et al. (2008) used the WRF model to simulate a hurricane and found that when the horizontal resolution increased from 4 to 1.3 km, the minimum sea level pressure changed by 20 hPa and the maximum wind speed increased by 13 m/s. Gentry and Lackmann (2010) used the WRF model to study the sensitivity of typhoon to horizontal grid spacing (1 to 8 km). It shows that after the resolution is increased, the central minimum pressure is significantly reduced. The above studies show that in typhoon simulation, horizontal resolution is the main reason for this difference compared to other factors (Fierro et al., 2009; Gall et al., 2011; Manganello et al., 2012; Walsh et al., 2013; Done et al., 2015). In order to reveal the difference in grid resolution on typhoon track and intensity, the sensitivity experiments with different horizontal resolutions, vertical resolutions and top pressure have been discussed in this study. The dynamics and microphysical structural characteristics of the typhoon largely determine the strength and precipitation intensity of the typhoon center (Wang and Wu, 2004; Rogers et al., 2006; Wang et al., 2012). Therefore, the solution of this problem helps to better simulate typhoon intensity, precipitation and microstructure characteristics, and provides a theoretical basis for improving the intensity prediction of typhoons.

2 Method and data

2.1 *Method*

The weather research and forecasting (WRF) model is the latest generation of mesoscale meteorological models jointly developed by the National Center for Atmospheric Research (NCAR) and the National Center for Environmental Prediction (NCEP, Skamarock and Klemp, 2008). The WRF model can be used to simulate global and regional climate change, atmospheric motion and air quality at different scales can also be used for typhoon, hurricane simulation and coupled simulation of air-sea, which is widely used and has surpassed the MM5 model and become the most popular mesoscale atmospheric model. Currently, the WRF model includes two different dynamic frameworks, ARW (the advanced research WRF) and NMM (the non-hydrostatic mesoscale model), which are maintained and developed by the NCAR and NCEP respectively. This study is based on the ARW framework in the WRF model to carry out typhoon simulation.

This model adopts a fully compressible non-hydrostatic model with Arakawa C grid in the horizontal direction and terrain-following quality coordinates in the vertical direction (Laprise, 1992).

The vertical coordinate of the WRF is defined as

$$\eta = (p_h - p_{ht})/\mu, \tag{1}$$

where $\mu = p_{hs} - p_{ht}$, p_h is the static equilibrium component of the pressure, p_{hs} and p_{ht} is the pressures at the bottom boundary (ground) and top boundary of the model, respectively.

The static vertical coordinate of terrain-following has been shown in Fig. 1. The value range η is between 0 to 1, and η in the bottom boundary is η=1, and the top boundary is η=0. This coordinate form is a traditional coordinate and is widely used in many static meteorological models.

The vertical direction uses the vertical-following static pressure vertical coordinate, and the Euler equations in the form of non-hydrostatic flux are as following:

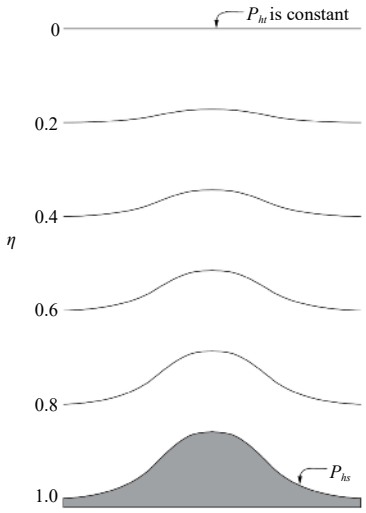

Fig. 1. Schematic diagram of terrain following vertical coordinates in WRF model.

$$\partial_t U + (\nabla \cdot V_u) - \partial_x (p\partial_\eta \varphi) + \partial_\eta (p\partial_\eta \varphi) = F_U, \tag{2}$$

$$\partial_t V + (\nabla \cdot V_v) - \partial_y (p\partial_\eta \varphi) + \partial_\eta (p\partial_y \varphi) = F_V, \tag{3}$$

$$\partial_t W + (\nabla \cdot V_w) - g(\partial_\eta p - \mu) = F_W, \tag{4}$$

$$\partial_t \Theta + (\nabla \cdot V_\theta) = F_\Theta, \tag{5}$$

$$\partial_t \mu + (\nabla \cdot V) = 0, \tag{6}$$

$$\partial_t \varphi + \mu^{-1}[(\nabla \cdot V_\varphi) - gW] = 0. \tag{7}$$

The equations need to satisfy the diagnostic relations of static equilibrium (Eq. (8)) and the gas state Eq. (9):

$$\partial_\eta \varphi = -\alpha\mu, \tag{8}$$

$$p = p_0 (R_d\theta/p_0\alpha)^\gamma, \tag{9}$$

where $V = \mu v = \mu(u, v, w)$, $\mu(x, y)$ represents the mass per unit area of the air column at the model grid point (x, y), $\Theta = \mu\theta$, θ is the potential temperature, $\varphi = gz$ is the potential, and p is the atmospheric pressure, p_0 is taken as the constant 1 000 hPa, and $\alpha = 1/\rho$ is the specific volume of air. γ is the ratio of the constant pressure specific heat and constant specific heat in dry air, which take γ=c_p/c_v= 1.4. In Eq. (2) to Eq. (5), the F_U, F_V, F_W and F_Θ in the right of the equation represent the source terms of forces generated by model physics, turbulent blending, spherical projection, and earth selection, respectively.

2.2 *Data*

Typhoon Kai-tak was the 13th typhoon in 2012 and formed a tropical depression on the eastern ocean of the Philippines on the evening of August 12, 2012. At about 08:00 on August 13, it

reached the southeastern ocean off the Taiwan Island (16.9°N, 127.8°E) and was continuously strengthened. The maximum wind speed in the center reached 18 m/s or above, and the lowest pressure was 998 hPa, and moved to the northwest with a speed around 10 km/h and gradually approached the southern ocean of Taiwan. The typhoon satellite image is shown in Fig. 2.

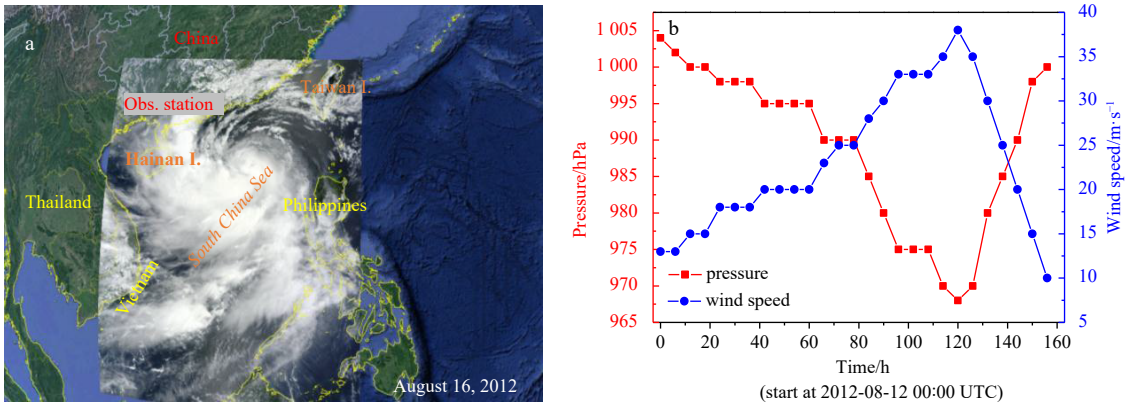

Fig. 2. Typhoon Kai-tak (2012). a. Satellite image and b. sea level pressure and wind speed.

At 05:00 on August 16, 2012, it was strengthened as a typhoon level over the north of the South China Sea. At the time of 06:00, the center of the typhoon was in the south of Zhanjiang, Guangdong Province (18.7°N, 118.2°E). The maximum wind speed near the center was more than 33 m/s, and the minimum pressure in the center is 975 hPa. It landed on Zhanjiang in Guangdong Province around 12:30 on August 17. At the time of landing, the maximum wind speed near the center was 38 m/s, and the minimum pressure in the center was 968 hPa. At 21:30 on August 17, it landed again on the China-Vietnam coast and began to weaken and gradually dissipated on the August 18. The Typhoon Kai-tak caused heavy rainfall in most parts of southern China and caused floods and other disasters, leading to serious losses in the affected areas.

The WRF model was used to simulate Typhoon Kai-tak, and the development and movement process of Kai-tak over the South China Sea region has been simulated (2012-08-15 00 UTC to 2012-08-18 06:00 UTC). The computational domain is the South China Sea and the East China Sea region (0°–32°N, 102°–130°E), as shown in Fig. 3.

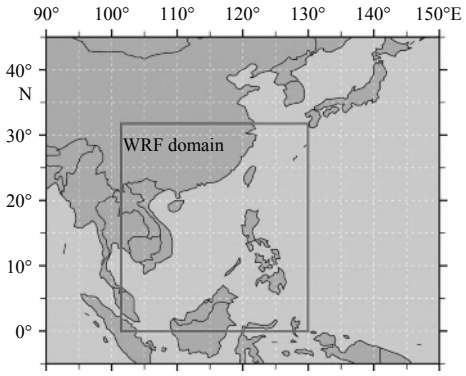

Fig. 3. The computational domain in this study.

The shoreline data comes from the global self-consistent, hierarchical, high-resolution shorelines (GSHHS) provided by the National Geophysical Data Center (NGDC, Wessel and Smith, 1996). The dataset provides 1:250 000 worldwide coastline data. The depth data used in this model comes from the 1-minute gridded global relief data collection (ETOPO1) provided by the NGDC. The dataset has a grid resolution of 1 minute. The coverage range is between 90°S–90°N and 180°W–180°E. The initial field and side boundary conditions of the WRF model are taken from the NCEP/NCAR reanalysis FNL data. The reanalysis FNL data provided by the NCEP/NCAR uses the GRIB format and contains 26 non-uniformly distributed pressure data from 1 000 hPa to 10 hPa. The time series of the FNL data has been updated since August in 1999. The data time interval is 6 hours, which means that the daily data includes 00:00, 06:00, 12:00 and 18:00 in one day. The spatial resolution of the data is 1.0°×1.0°. The physical and parameterization schemes for Typhoon Kai-tak in the WRF has been shown in Table 1.

The case study of Kai-tak (1213) used the single-moment 6-class microphysics (WSM6) scheme for micro-physical processes (Hong and Lim, 2006). The Kain-Fritsch (KF-Eta, (Kain, 2004)) scheme for cumulus convection, the Yonsei University (YSU; Hong et al. (2006)) scheme for PBL processes, rapid radiation transfer model (RRTM) for long wave radiation (Mlawer et al., 1997) and Dudhia (1989) scheme for shortwave parameters.

2.3 *Evaluation method*

In order to more comprehensively evaluate the influence of different schemes on the simulation effect of typhoon track and intensity, the root mean square error (*RMSE*) and Pearson correlation coefficient (*R*) have been selected to be the evaluation parameters for the typhoon track and intensity is analyzed in this study.

The formula of the *RMSE* and *R* are as follows:

$$RMSE = \sqrt{\frac{\sum_{i=1}^{n}(x_i - y_i)^2}{n}}, \tag{10}$$

$$R = \frac{\sum_{i=1}^{n}(x_i - \overline{x_i})(y_i - \overline{y_i})}{\sqrt{\sum_{i=1}^{n}(x_i - \overline{x_i})^2}\sqrt{\sum_{i=1}^{n}(y_i - \overline{y_i})^2}}, \tag{11}$$

Table 1. The overview of model configuration

Item	Configuration
Model	WRF V3.9.1
Simulation time	78 h (2012-08-15 00:00 UTC to 2012-08-18 06:00 UTC)
Micro-physics scheme	the WRF Single-Moment 6-Class Microphysics (WSM6) scheme
Planetary boundary scheme	Yonsei University (YSU) scheme
Land surface parameterization	Noah land surface scheme
Long wave radiation scheme	rapid Radiative Transfer Model (RRTM) scheme
Short wave radiation scheme	Dudhia scheme
Cumulus convective scheme	Kain-Fritsch (K-F) scheme
Horizontal resolution	Exp. 1: 5 km; Exp. 2: 10 km; Exp. 3: 20 km; Exp. 4: 30 km; Exp. 5: 5 km+15 km (nesting)
Vertical resolution	Exp. 1: 35; Exp. 2: 28; Exp. 3: 20
Top pressure	Exp. 1: 1 000 Pa; Exp. 2: 2 000 Pa; Exp. 3: 3 500 Pa; Exp. 4: 5 000 Pa

where n is the number of the simulation results, x_i is the simulation result, $\overline{x_i}$ is the average of the simulation results, y_i is the observation result, and $\overline{y_i}$ is the average of the observations.

3 Results and discussion

3.1 *The effect of horizontal resolution*

3.1.1 *Horizontal resolution without nesting*

According to previous research results, horizontal resolution is one of the main impact factors affecting the track and intensity of typhoon simulation. With the development of computer technology, the horizontal resolution of the mesoscale meteorological model has developed from 100 km to 10 km to 1 km today. During the period of development, the simulation results have been continuously improved. The effect of horizontal resolution on the simulated typhoon track and intensity based on the WRF model has been discussed in this section.

It can be seen from Fig. 4 to Fig. 6 that the improvement of horizontal resolution can improve the accuracy of typhoon simulation. In terms of typhoon track, the effect of horizontal resolution is relatively limited, but in wind speed simulation, the higher the horizontal resolution, the more obvious the improvement of the simulation accuracy of the wind speed.

It is well known that the atmospheric movement under the influence of typhoons is essentially the result of the combined effects of different physical quantities at multiple time and space scales. In the mesoscale meteorological model, the improvement of horizontal resolution will inevitably have stronger and better fitting ability and effect on the simulation of these physical processes. Therefore, improving the horizontal resolution of the mesoscale meteorological model is more accurate for the simulation of atmospheric dynamic processes and climate systems in the corresponding space-time scales. At the same time, the increase in horizontal resolution will inevitably lead to an increase in the amount of calculation, which will increase the calculation time and reduce the calculation efficiency. Therefore, it is necessary to make a reasonable balance between calculation accuracy and calculation efficiency.

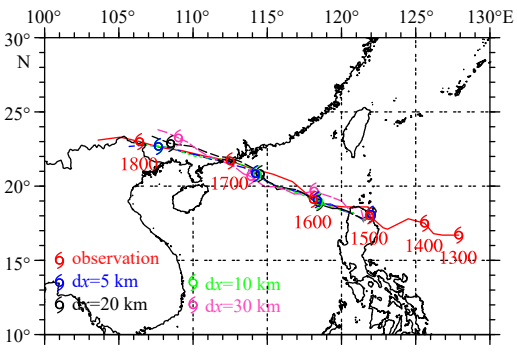

Fig. 4. Comparison of Typhoon Kai-tak track simulation under different horizontal resolution conditions. dx is the horizontal resolution.

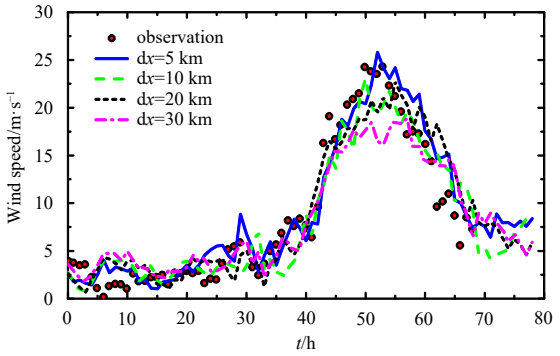

Fig. 5. Comparison of Typhoon Kai-tak strength under different horizontal resolution conditions (start at 2012–08–15 00:00 UTC).

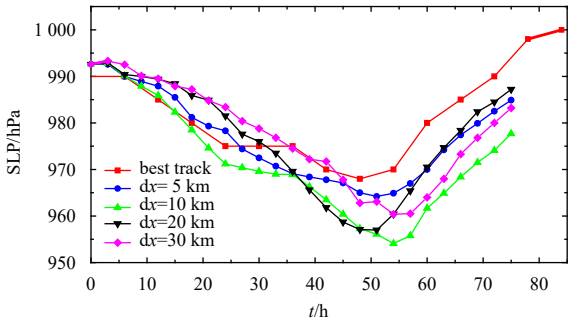

Fig. 6. Comparison of Typhoon Kai-tak intensity under different horizontal resolution conditions (start at 2012–08–15 00:00 UTC).

3.1.2 *Horizontal resolution with nesting*

In the previous study, we found that the accuracy of the horizontal resolution can be improved to obtain more accurate simulation results, but at the same time, the increase in resolution leads to a large increase in the amount of numerical calculation, the calculation time increases and the calculation efficiency de-

creases. Therefore, how to balance the calculation accuracy and calculation efficiency is an important issue to be considered in the numerical simulation based on the WRF model. Grid nesting technology is an effective way to solve this problem. A coarser-resolution grid is used to calculate in a large-scale calculation area, and a higher-resolution grid is used in the calculation area of the main concern. Through this nested grid method, it can obtain high calculation accuracy in the key area of interest and ensure reasonable calculation efficiency in the whole computational domain.

(1) Nesting technique in WRF

In the WRF model, horizontal grids of multiple regions can be used for nesting. The horizontal grid nesting method can be divided into one-way simulation and two-way simulation. As shown in Fig. 7, the integral calculation of the higher-resolution grid does not affect the coarser-resolution grid when one-way nesting, that is, only the data of the coarser-resolution grid is transferred to the higher-resolution grid, and the calculation result of the higher-resolution grid is not transmitted back to the coarser-resolution grid. When using two-way nesting, mutual data feedback is needed between the coarser-resolution grid and the higher-resolution grid. The two-way nesting for numerical calculation has been used in this study.

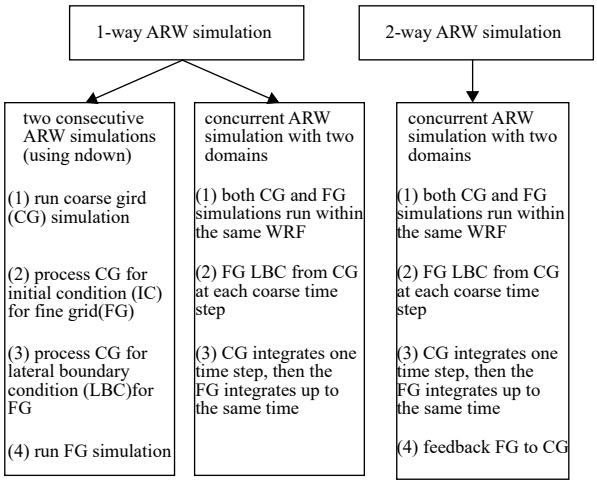

Fig. 7. Schematic diagram of one-way nesting and two-way nesting in the WRF model.

In general, the nesting of multiple grids includes the following types as shown in Fig. 8: Fig. 8a is a strict layer-layer nesting grid, that is, each child grid is included in the parent grid; Fig. 8b indicates that under a certain level of the parent grid, two or more juxtaposed child grids may be included, but the child grids are independent of each other; Fig. 8c indicates that there are two or more juxtaposed child grids under a certain parent grid, but there is an overlapping zone between the child grids; Fig. 8d indicates that the parent grid contains two or more juxtaposed child grids, and the juxtaposed child grids contain internal grids. In the WRF model, the two nesting grids shown in Figs 8c and d are not allowed. In this study, the first type of grid nesting is used, that is, a strict layer-layer nesting grid has been used in this paper.

(2) Application of two-way nesting grid

In this paper, two sets of two-way nesting grids and non-nesting grids are set up, as shown in Table 1. The computational domain and grid nesting range of the two-way nesting grid are shown in Fig. 9. From the aspects of simulation accuracy and

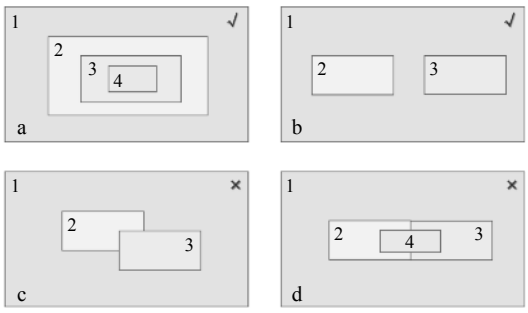

Fig. 8. Schematic diagram of different types of multi-grid nesting.

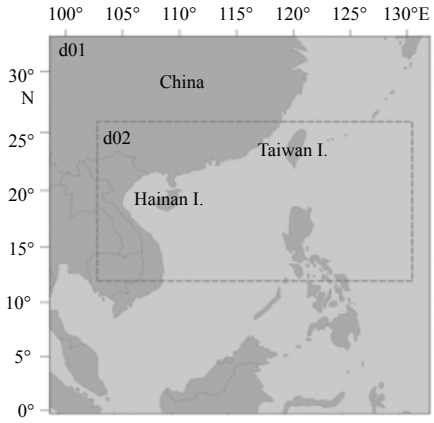

Fig. 9. Schematic diagram of the computational domain of Typhoon Kai-tak based on nesting grid.

simulation efficiency, according to the analysis of the simulation results of typhoon track and intensity, the nesting calculation method of horizontal resolution using 15 km and 5 km grid resolution for data translating is determined, as shown in Fig. 9. The space step of the child grid is 1/3 of the parent grid space step, which are 5 km and 15 km, respectively. The child grid time step is 3 times the parent grid time step.

The simulation results of typhoon track, strength and intensity under different nesting conditions have been shown in Fig. 10 to Fig. 12. As shown in the figures, the use of nesting grids improves the accuracy of typhoon simulation. In terms of typhoon track, the effect of horizontal resolution is relatively limited, but in the simulation of wind speed and air pressure, the calculated results based on the nesting grids are close to those calculated using the 5 km grid resolution. It can be seen that the use of nesting grids can improve computational accuracy to a large extent while saving computation time.

3.2 *The effect of vertical resolution*

3.2.1 *Effect of vertical layers*

The effect of horizontal grid resolution on the simulation results is discussed in Section 3.1. Corresponding to the horizontal grid resolution, the vertical layers (e_vert-1) in the WRF model also affects the simulation results. This section discusses and analyzes the effects of different vertical layers in typhoon simulation. Similar to the horizontal resolution, the increase in the number of vertical layers will lead to an increase in the calculation of the WRF model. Therefore, in the simulation process of

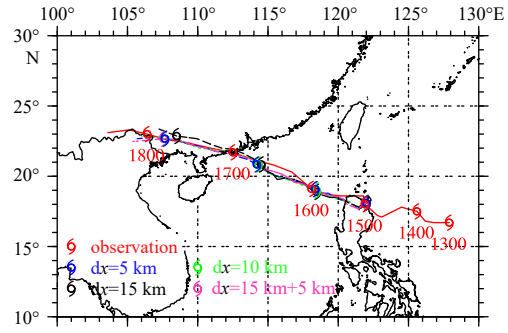

Fig. 10. Comparison of Typhoon Kai-tak track simulation under different nesting resolution conditions.

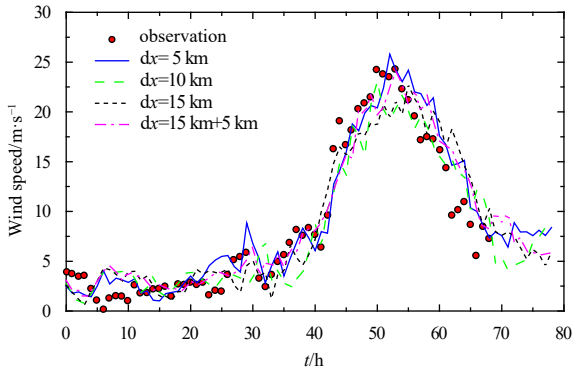

Fig. 11. Comparison of Typhoon Kai-tak strength under different nesting resolution conditions (start at 2012–08–15 00:00 UTC).

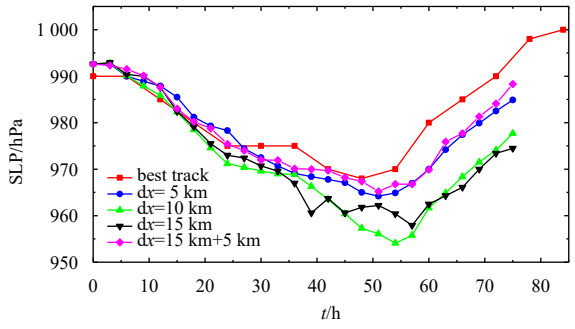

Fig. 12. Comparison of Typhoon Kai-tak intensity under different nesting resolution conditions (start at 2012–08–15 00:00 UTC).

the typhoon track, strength and intensity, the appropriate number of vertical layers is selected to ensure the simulation accuracy of the model.

Under the same conditions, the typhoon Kai-tak simulation conditions in the experiments of vertical layer number of 20-layers, 28-layers and 35-layers are set respectively. The simulation results of typhoon track, strength and intensity under different conditions are obtained by calculation, and the simulation results in three experiments are compared with the observed data of the station. The observation station is shown in Fig. 2, and the comparison results are shown in Fig. 13 to Fig. 15.

It can be seen from Fig. 13 to Fig. 15 that the change of the number of vertical layers has an influence on the track, strength

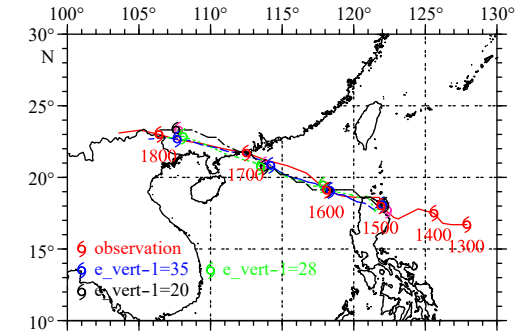

Fig. 13. Comparison of Typhoon Kai-tak track simulation under different vertical layers.

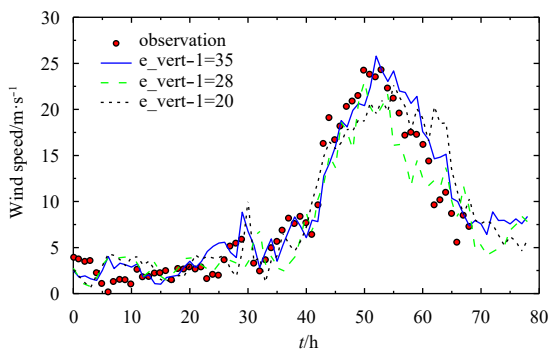

Fig. 14. Comparison of Typhoon Kai-tak strength under different vertical layers (start at 2012–08–15 00:00 UTC).

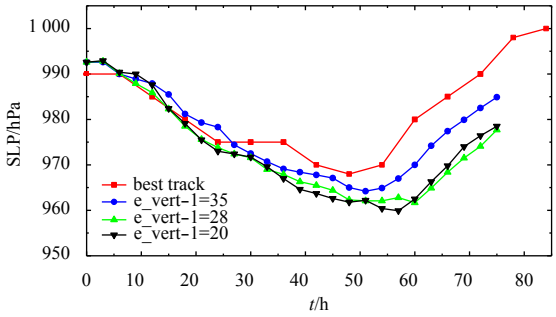

Fig. 15. Comparison of Typhoon Kai-tak intensity under different vertical layers (start at 2012–08–15 00:00 UTC).

and intensity simulation of the Typhoon Kai-tak. In the wind speed simulation of the Typhoon Kai-tak, during the period when the typhoon wind speed is large, the wind speed extreme value obtained by the simulation of the 20-layers and 28-layers has a significant deviation from the observed value; and the simulated wind speed extreme value agrees well with the measured results when using 35-layers in the WRF model.

In the simulation of the lowest SLP (sea level pressure) in the center, the simulation results under the three conditions are smaller than the observed results, that is, the intensity simulation is stronger than the observation. The simulation and observation are relatively close when the vertical layer is 35-layers. In the track simulation of Typhoon Kai-tak, when the number of layers is 35-layers and 28-layers, both show good simulation results. In general, when simulating the Typhoon Kai-tak, the vertical resolution using 35-layer simulation results is better than the

simulation results using 20-layer and 28-layer simulations. Therefore, in the simulation of the Typhoon Kai-tak in this paper, the recommended number of layers is 35-layers.

Through the above analysis, it can be found that when the Typhoon Kai-tak is numerically simulated by the WRF model, the larger the number of the vertical layers is, the higher the simulation accuracy is. However, some scholars found that the vertical resolution in the WRF model, the vertical resolution should be based on background data and wind conditions to select the appropriate number of vertical layers, rather than the vertical layer as much as possible. Therefore, it can be thought that the more the vertical layers in the WRF model, the higher the simulation accuracy, when it is suitable for the corresponding background field and driving conditions.

3.2.2 *Effect of top pressure*

Since in the mesoscale atmospheric model WRF, the isostatic line is layered by the σ coordinate in the vertical direction, when the number of vertical layers is constant, if the top maximum pressure is larger, at this time, the calculation accuracy on the vertical resolution is correspondingly smaller, so the top maximum pressure (p_top) has an important influence on the simulation results. Therefore, the top maximum pressure is also one of the factors that affect the vertical resolution using the WRF model.

In order to further carry out the vertical resolution sensitivity analysis in the Typhoon Kai-tak simulation process, in the experiment of the same selection of other parameters, the top maximum pressure is calculated as 1 000 Pa, 2 000 Pa, 3 500 Pa and 5 000 Pa, respectively. The situation and simulation conditions are shown in Table 1. Through the calculation, the simulation results obtained under the four conditions are compared with the observed data. The observation station is shown in Fig. 2. The comparison between the typhoon track, the wind speed and the central minimum pressure is shown in Fig. 16 to Fig. 18.

It can be seen from Fig. 16 to Fig. 18 that for the Typhoon Kai-tak, the different conditions of the top maximum pressure have an influence on the track, strength and intensity of the Typhoon Kai-tak. In the simulation period with large wind speed, the wind speed when the top maximum pressure is taken as 5 000 Pa is significantly smaller than the simulation result when the top maximum pressure is taken as 2 000 Pa and 3 500 Pa. When the top maximum pressure is 1 000 Pa, the calculated wind speed is slightly larger than the observed value, while the calculation results at the top maximum pressure of 2 000 Pa and 3 500 Pa are close, and the matching with the observed values is better. In the large wind speed period, the wind speed value when the top maximum pressure is 2 000 Pa is more accurate than the wind

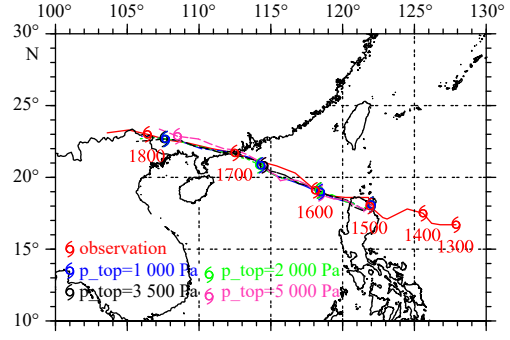

Fig. 16. Comparison of Typhoon Kai-tak track simulation under different top maximum pressure.

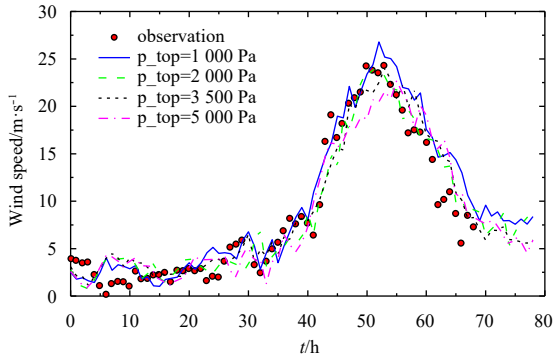

Fig. 17. Comparison of Typhoon Kai-tak strength under different top maximum pressure (start at 2012–08–15 00:00 UTC).

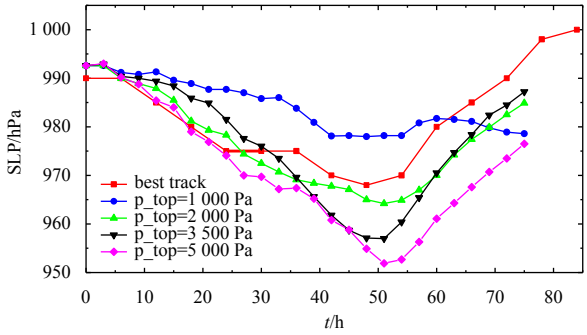

Fig. 18. Comparison of Typhoon Kai-tak intensity under different top maximum pressure (start at 2012–08–15 00:00 UTC).

speed value when the top maximum pressure is 3 500 Pa. Considering that during the simulation of the Typhoon Kai-tak, the wind speed when the top maximum pressure is 2 000 Pa is in good agreement with the observed results. Therefore, in the following simulation of Typhoon Kai-tak, the top maximum pressure is recommended to be 2 000 Pa.

3.3 *Results of typhoon field*

From the previous analysis, it is known that there are many influencing factors affecting the typhoon track, strength and intensity. The sensitivity of the above parameters is explored by systematically analyzing the influence of horizontal resolution and vertical resolution on the typhoon simulation accuracy using the atmospheric model WRF. From the aspects of simulation accuracy and simulation efficiency, and from the simulation results of typhoon track, strength and intensity, the nesting grid method of horizontal resolution using two-way nesting grid of 15 km and 5 km is comprehensively determined, and the vertical layers are 35-layers, the top maximum pressure is 2 000 Pa. Using the above simulation scheme, the wind field distribution and pressure field distribution results under the influence of the Typhoon Kai-tak are obtained, as shown in Figs 19 and 20, respectively.

From the numerical results, it can be seen that from 2012–08–15 12:00 to 2012–08–17 06:00 UTC, the Typhoon Kai-tak gradually strengthened and gradually approached the coastal ocean of Guangdong. During this period, the coastal areas of Guangdong were dominated by north wind and northeast wind, and a strong wind zone is formed near the west of the Pearl River Estuary. With the further strengthening of the Typhoon Kai-tak and the movement to the northwest, the offshore zone near the

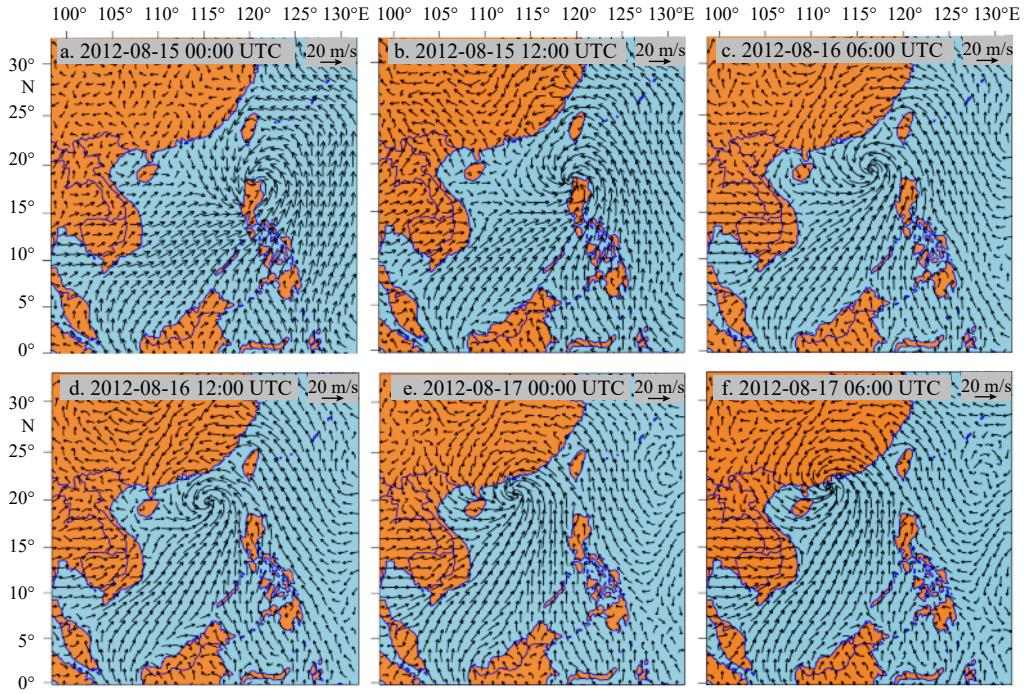

Fig. 19. The wind field of Typhoon Kai-tak based on the WRF model.

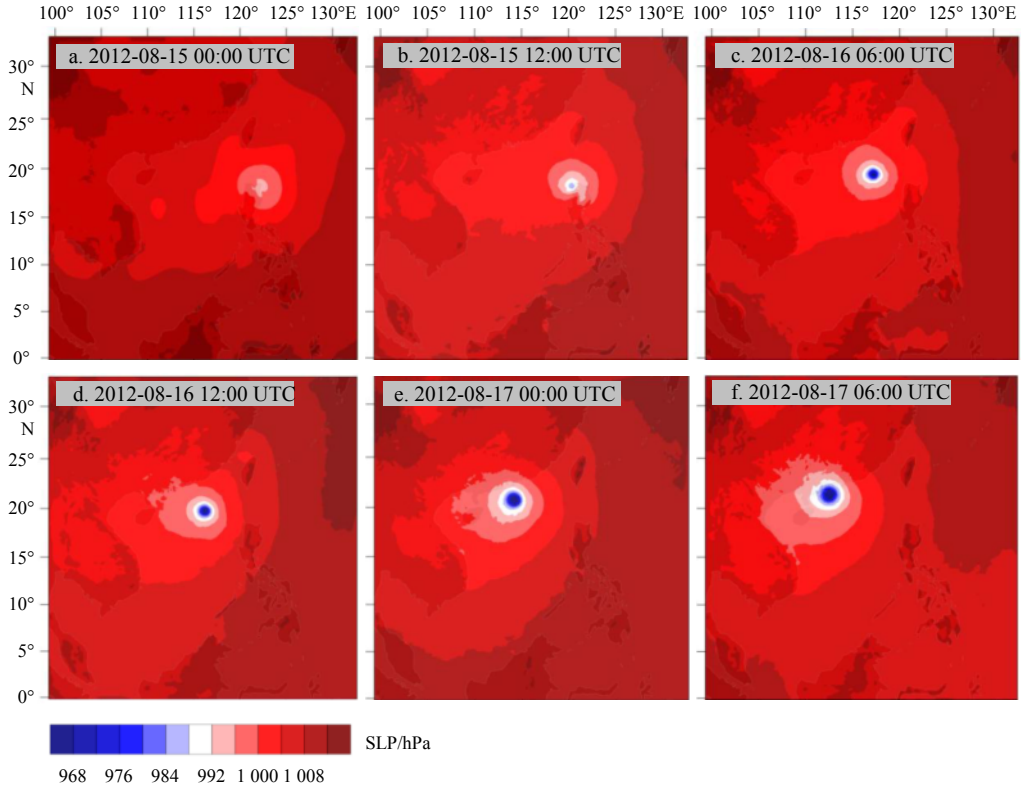

Fig. 20. The pressure field of Typhoon Kai-tak based on the WRF model.

east of Shantou has been controlled by the maximum wind speed zone near the typhoon center, and the wind field is very strong. It can be found that the Typhoon Kai-tak center obtained by WRF simulation landfall at around 2012–08–17 06:00 UTC, which is about 3 hours later than the actual landfalling time. This indicates that the simulated typhoon movement speed is slower than the actual situation, which is also the reason why the simulated typhoon moving speed results are slower, the intensity is larger, and the wind speed is larger than the observed results.

4 Conclusions

In order to reasonably determine the grid parameters of the

WRF model in the typhoon simulation, the Typhoon Kai-tak as an example had been used to analyze the sensitivity of horizontal resolution, nesting grid, vertical layers and top maximum pressure in the simulation results of track, strength and intensity. Different horizontal resolutions (5, 10, 20, 30 km), nesting grids (15 and 5 km), different vertical resolutions (35-layers, 28-layers, 20-layers) and different top maximum pressures (1 000 Pa, 2 000 Pa, 3 500 Pa, 5 000 Pa) had been used in the mesoscale numerical model WRF to simulate the Typhoon Kai-tak. By comparing and analyzing the simulation results at different horizontal and vertical resolutions, the following conclusions can be drawn.

(1) The horizontal resolution of the model has a limit effect on the simulation effect of the typhoon track, and the model at each resolution can better simulate the track of the typhoon. Different horizontal resolutions have different simulation effects on typhoon strength (defined by wind speed) and intensity (defined by sea level pressure, SLP), especially for sea level pressure. The typhoon intensity simulated by the high-resolution model is closer to the real situation. The nesting grids can improve computational accuracy while saving computation time.

(2) The vertical resolution included vertical layers and top maximum pressure of the model also has limited effect on the simulation effect of the typhoon track, but have obvious effects on typhoon strength and intensity. The typhoon intensity simulated by the high-resolution model is closer to the real situation. The nesting grids can improve computational accuracy while saving computation time. The simulation results affected by vertical resolution using 35-layers is better than the simulation results using 20-layers and 28-layers simulations.

Through comparison and analysis, the horizontal and vertical resolutions of WRF model are finally determined by the simulation accuracy, simulation efficiency, and the simulation results of typhoon track, strength and intensity as follows: the two-way nesting grid of 15 km and 5 km is comprehensively determined, and the vertical layers is 35-layers, the top maximum pressure is 2 000 Pa. It should be noted that the conclusions of this paper are obtained under specific individual cases and physical process conditions. If different parameterization schemes or different examples are adopted, the results may be different. More statistical analysis is needed to obtain conclusions of general significance.

References

Bacmeister J T, Reed K A, Hannay C, et al. 2018. Projected changes in tropical cyclone activity under future warming scenarios using a high-resolution climate model. Climatic Change, 146(3–4): 547–560, doi: 10.1007/s10584-016-1750-x

Davis C, Wang Wei, Chen S S, et al. 2008. Prediction of landfalling hurricanes with the advanced hurricane WRF model. Monthly Weather Review, 136(6): 1990–2005, doi: 10.1175/2007MWR2085.1

Done J M, Holland G J, Bruyère C L, et al. 2015. Modeling high-impact weather and climate: lessons from a tropical cyclone perspective. Climatic Change, 129(3–4): 381–395, doi: 10.1007/s10584-013-0954-6

Dudhia J. 1989. Numerical study of convection observed during the winter monsoon experiment using a mesoscale two-dimensional model. Journal of the Atmospheric Sciences, 46(20): 3077–3107, doi: 10.1175/1520-0469(1989)046<3077:NSOCOD>2.0.CO;2

Fierro A O, Rogers R F, Marks F D, et al. 2009. The impact of horizontal grid spacing on the microphysical and kinematic structures of strong tropical cyclones simulated with the WRF-ARW model. Monthly Weather Review, 137(11): 3717–3743, doi: 10.1175/2009MWR2946.1

Gall J S, Ginis I, Lin S J, et al. 2011. Experimental tropical cyclone prediction using the GFDL 25-km-resolution global atmospheric model. Weather and Forecasting, 26(6): 1008–1019, doi: 10.1175/WAF-D-10-05015.1

Gentry M S, Lackmann G M. 2010. Sensitivity of simulated tropical cyclone structure and intensity to horizontal resolution. Monthly Weather Review, 138(3): 688–704, doi: 10.1175/2009MWR2976.1

Gettelman A, Bresch D N, Chen C C, et al. 2018. Projections of future tropical cyclone damage with a high-resolution global climate model. Climatic Change, 146(3–4): 575–585, doi: 10.1007/s10584-017-1902-7

Guo Xingliang, Zhong Wei. 2017. The use of a spectral nudging technique to determine the impact of environmental factors on the track of typhoon megi (2010). Atmosphere, 8(12): 257, doi: 10.3390/atmos8120257

Hendricks E A, Jin Yi, Moskaitis J R, et al. 2016. Numerical simulations of Typhoon Morakot (2009) using a multiply nested tropical cyclone prediction model. Weather and Forecasting, 31(2): 627–645, doi: 10.1175/WAF-D-15-0016.1

Hong S Y, Lim J O J. 2006. The WRF single-moment 6-class microphysics scheme (WSM6). Journal of the Korean Meteorological Societys, 42(2): 129–151

Hong S Y, Noh Y, Dudhia J. 2006. A new vertical diffusion package with an explicit treatment of entrainment processes. Monthly Weather Review, 134(9): 2318–2341, doi: 10.1175/MWR3199.1

Jun S, Kang N Y, Lee W, et al. 2017. An alternative multi-model ensemble forecast for tropical cyclone tracks in the western North Pacific. Atmosphere, 8(9): 174, doi: 10.3390/atmos8090174

Kain J S. 2004. The Kain-Fritsch convective parameterization: an update. Journal of Applied Meteorology, 43(1): 170–181, doi: 10.1175/1520-0450(2004)043<0170:TKCPAU>2.0.CO;2

Knutson T R, McBride J L, Chan J, et al. 2010. Tropical cyclones and climate change. Nature Geoscience, 3(3): 157–163, doi: 10.1038/ngeo779

Laprise R. 1992. The euler equations of motion with hydrostatic pressure as an independent variable. Monthly Weather Review, 120(1): 197–207, doi: 10.1175/1520-0493(1992)120<0197:TEEOMW>2.0.CO;2

Li Funing, Song Jinbao, Li Xia. 2018. A preliminary evaluation of the necessity of using a cumulus parameterization scheme in high-resolution simulations of Typhoon Haiyan (2013). Natural Hazards, 92(2): 647–671, doi: 10.1007/s11069-018-3218-y

Manganello J V, Hodges K I, Kinter III J L, et al. 2012. Tropical cyclone climatology in a 10-km global atmospheric GCM: toward weather-resolving climate modeling. Journal of Climate, 25(11): 3867–3893, doi: 10.1175/JCLI-D-11-00346.1

Mlawer E J, Taubman S J, Brown P D, et al. 1997. Radiative transfer for inhomogeneous atmospheres: RRTM, a validated correlated-k model for the longwave. Journal of Geophysical Research: Atmospheres, 102(D14): 16663–16682, doi: 10.1029/97JD00237

Rogers R, Aberson S, Black M, et al. 2006. The intensity forecasting experiment: a NOAA multiyear field program for improving tropical cyclone intensity forecasts. Bulletin of the American Meteorological Society, 87(11): 1523–1537, doi: 10.1175/BAMS-87-11-1523

Skamarock W C, Klemp J B. 2008. A time-split nonhydrostatic atmospheric model for weather research and forecasting applications. Journal of Computational Physics, 227(7): 3465–3485, doi: 10.1016/j.jcp.2007.01.037

Sun Yuan, Zhong Zhong, Li T, et al. 2017. Impact of ocean warming on tropical cyclone track over the western north pacific: a numerical investigation based on two case studies. Journal of Geophysical Research: Atmospheres, 122(16): 8617–8630, doi: 10.1002/2017JD026959

Walsh K, Lavender S, Scoccimarro E, et al. 2013. Resolution dependence of tropical cyclone formation in CMIP3 and finer resolution models. Climate Dynamics, 40(3–4): 585–599, doi: 10.1007/s00382-012-1298-z

Wang C C, Kuo H C, Chen Yuhan, et al. 2012. Effects of asymmetric latent heating on typhoon movement crossing Taiwan: the case of Morakot (2009) with extreme rainfall. Journal of the Atmospheric Sciences, 69(11): 3172–3196, doi: 10.1175/JAS-D-11-

0346.1

Wang Hui, Wang Yuqing. 2014. A numerical study of Typhoon Megi (2010). Part I: rapid intensification. Monthly Weather Review, 142(1): 29–48, doi: 10.1175/MWR-D-13-00070.1

Wang Y, Wu C C. 2004. Current understanding of tropical cyclone structure and intensity changes-a review. Meteorology and Atmospheric Physics, 87(4): 257–278, doi: 10.1007/s00703-003-0055-6

Weisman M L, Skamarock W C, Klemp J B. 1997. The resolution dependence of explicitly modeled convective systems. Monthly Weather Review, 125(4): 527–548, doi: 10.1175/1520-0493(1997)125<0527:TRDOEM>2.0.CO;2

Weng C H, Hsu H H. 2017. Intraseasonal oscillation enhancing C5 typhoon occurrence over the tropical western North Pacific. Geophysical Research Letters, 44(7): 3339–3345, doi: 10.1002/2017GL072743

Wessel P, Smith W H F. 1996. A global, self-consistent, hierarchical, high-resolution shoreline database. Journal of Geophysical Research: Solid Earth, 101(B4): 8741–8743, doi: 10.1029/96JB00104

Wu Zhiyuan, Jiang Changbo, Chen Jie, et al. 2019a. Three-dimensional temperature field change in the south China Sea during typhoon Kai-tak (1213) based on a fully coupled atmosphere-wave-ocean model. Water, 11(1): 140, doi: 10.3390/w11010140

Wu Zhiyuan, Jiang Changbo, Deng Bin, et al. 2018. Evaluation of numerical wave model for typhoon wave simulation in South China Sea. Water Science and Engineering, 11(3): 229–235, doi: 10.1016/j.wse.2018.09.001

Wu Zhiyuan, Jiang Changbo, Deng Bin, et al. 2019b. Numerical investigation of Typhoon Kai-tak (1213) using a mesoscale coupled WRF-ROMS model. Ocean Engineering, 175: 1–15, doi: 10.1016/j.oceaneng.2019.01.053

Wu Zhiyuan, Jiang Changbo, Mack C, et al. 2019c. Hybrid improved empirical mode decomposition and BP neural network model for the prediction of sea surface temperature. Ocean Science, 15(2): 349–360, doi: 10.5194/os-15-349-2019